World Journal of Urology (2024) 42:46
https://doi.org/10.1007/s00345-023-04746-9

TOPIC PAPER

Advancements in stone classification: unveiling the beauty of urolithiasis

Vincent De Coninck[1,2] · Andreas Skolarikos[3] · Patrick Juliebø-Jones[4] · Manu Joris[5] · Olivier Traxer[6,7] · Etienne Xavier Keller[2,8]

Received: 23 September 2023 / Accepted: 2 November 2023
© The Author(s), under exclusive licence to Springer-Verlag GmbH Germany, part of Springer Nature 2024

Abstract

Purpose Urolithiasis has become increasingly prevalent, leading to higher disability-adjusted life years and deaths. Various stone classification systems have been developed to enhance the understanding of lithogenesis, aid urologists in treatment decisions, and predict recurrence risk. The aim of this manuscript is to provide an overview of different stone classification criteria.

Methods Two authors conducted a review of literature on studies relating to the classification of urolithiasis. A narrative synthesis for analysis of the studies was used.

Results Stones can be categorized based on anatomical position, size, medical imaging features, risk of recurrence, etiology, composition, and morphoconstitutional analysis. The first three mentioned offer a straightforward approach to stone classification, directly influencing treatment recommendations. With the routine use of CT imaging before treatment, precise details like anatomical location, stone dimensions, and Hounsfield Units can be easily determined, aiding treatment planning. In contrast, classifying stones based on risk of recurrence and etiology is more complex due to dependencies on multiple variables, including stone composition and morphology. A classification system based on morphoconstitutional analysis, which combines morphological stone appearance and chemical composition, has demonstrated its value. It allows for the rapid identification of crystalline phase principles, the detection of crystalline conversion processes, the determination of etiopathogenesis, the recognition of lithogenic processes, the assessment of crystal formation speed, related recurrence rates, and guidance for selecting appropriate treatment modalities.

Conclusions Recognizing that no single classification system can comprehensively cover all aspects, the integration of all classification approaches is essential for tailoring urolithiasis patient-specific management.

Keywords Classification · Endourology · RIRS · SWL · Review · Ureteroscopy · Urolithiasis

✉ Vincent De Coninck
vincent.de.coninck@klina.be

1 Department of Urology, Augustijnslei 100, Klina, 2930 Brasschaat, AZ, Belgium

2 Young Academic Urologists (YAU), Urolithiasis and Endourology Working Party, Arnhem, The Netherlands

3 Department of Urology, National and Kapodistrian University of Athens, Athens, Greece

4 Department of Urology, Haukeland University Hospital, Bergen, Norway

5 Faculty of Medicine, University Hospitals Leuven, Louvain, Belgium

6 GRC N°20, Groupe de Recherche Clinique sur la Lithiase Urinaire, Hôpital Tenon, Sorbonne Université, Arnhem, The Netherlands

7 Service d'Urologie, Assistance-Publique Hôpitaux de Paris, Hôpital Tenon, Sorbonne Université, Arnhem, The Netherlands

8 Department of Urology, University Hospital Zurich, University of Zurich, Zurich, Switzerland

Published online: 20 January 2024

Introduction

Urolithiasis affects a significant proportion of the global population, with prevalence rates ranging between 1 and 13% worldwide [1]. Since 1990, there has been a rise in the overall number of urolithiasis cases, as well as the associated disability-adjusted life years and deaths [2, 3]. This underscores the importance of implementing diverse strategies aimed at preventing and treating urolithiasis.

To support urologists in making treatment decisions, identifying the characteristics of stones, deepening the understanding of lithogenesis, and predicting the risk of recurrence, various stone classification systems have been developed by guidelines committees [4, 5]. The aim of this manuscript is to provide an overview of different stone classification criteria to facilitate better understanding stone formation, guide treatment strategies, and prevent stone recurrence.

Methods

Two authors (V.D.C. and E.X.K.) conducted a review of literature using the Medline, Scopus, and Web of Science databases in July 2023. The search terms "classification" AND ("urolithiasis" OR "kidney stones") AND ("anatomy" OR "size" OR "imaging" OR "recurrence" OR "etiology" OR "composition" OR "morphoconstitutional analysis") were used, and the filters "English" and "humans" were applied. Only studies relating to the classification of urolithiasis were considered. Case reports, editorials, and letters were excluded. Additional articles identified through references lists were also included. A narrative synthesis for analysis of the studies was used. The content and structure of the manuscript were agreed upon by consensus between the two authors (V.D.C. and E.X.K.) (Table 1).

Results

Anatomical position

Urinary stones can be situated in diverse anatomical locations within the urinary tract, such as the pyelocaliceal system, ureter, bladder, or urethra (Fig. 1). To further pinpoint the location, the renal pelvis is considered as an important location of its own, as are the upper, middle, and lower calyces. The ureter is segmented into proximal, middle, and distal portions. The proximal ureter ranges from the ureteropelvic junction until the superior crest of the sacroiliac joint. The mid-ureter ranges from the superior to inferior

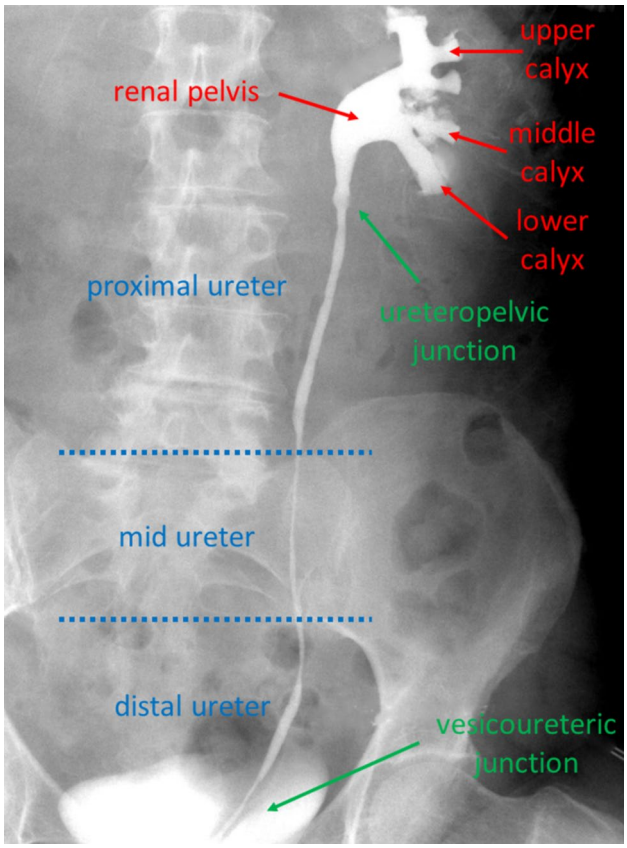

Fig. 1 Anatomy of the urinary system

crest of the sacroiliac joint. From there, the distal ureter passes through the vesicoureteric junction into the bladder. [6].Such precision in localization plays a pivotal role in selecting appropriate treatment modalities, ranging from conservative approaches to surgical intervention [4, 5, 7, 8].

Size

Stone size can be described using one, two, or three dimensions. The majority of literature reports stone burden based on the largest diameter, with stratification methods such as < 5 mm, 5–10 mm, 10–20 mm, and > 20 mm aiding in outcome comparison and treatment guidance [4, 5, 7–9]. This unidimensional measurement is arguably adequate for the description of small particles [10]. A minority of publications report stone size in surface area which can be calculated from both ultrasound (US) and kidney–ureter–bladder (KUB) radiography [9]. Finally, only a few publications report stone burden in terms of volume. This calculation method is on the rise for several reasons. Most patients receive non-contrast computerized tomography (CT). Reporting stone volume is undeniably the most accurate method for reporting stone burden [9]. It also allows the

assessment of stone ablation efficiency during laser lithotripsy [11]. With the development of thulium fiber lasers and devices with integrated pressure-measuring and aspiration technology, it also pushes boundaries of retrograde intrarenal surgery for larger stones [12, 13]. To facilitate stone burden measurements, fully automated systems for kidney stone detection and volume quantification on CT have been developed recently [14].

Medical imaging characteristics

US, KUB, and CT stand out as the most frequently employed imaging techniques for the comprehensive evaluation of urolithiasis. Depending on the mineral composition, stones can be categorized based on their appearance on plain X-rays, resulting in classifications such as radiopaque (including calcium oxalate monohydrate (whewellite), calcium oxalate dihydrate (weddellite), and brushite), poorly opaque (comprising carbapatite, magnesium ammonium phosphate (struvite), and cystine), or radiolucent (encompassing uric acid, urate, and miscellaneous types). In both single-energy and dual-energy CT scans, the Hounsfield Unit (HU) values have demonstrated predictive capabilities for determining stone compositions (Fig. 2) [15–21]. The lowest HU values (approximately 400) have been notably associated with uric acid stones, showing a remarkably high success rate in oral chemolysis treatment [22]. Additionally, investigations have revealed that lower HU values are linked to heightened success rates in shockwave lithotripsy (SWL), while higher HU values have exhibited a strong correlation with SWL failure [23–25].

Artificial intelligence presents as a valuable tool in the field of urolithiasis imaging, a topic commonly known as radiomics. Several studies to date have unveiled the potential of radiomics, suggesting that radiomics has a high potential to help clinicians providing personalized medicine [26].

Risk of recurrence

Accurately estimating the risk of stone recurrence is a significant concern, as it plays a pivotal role in safeguarding patients from potential regrowth, episodes of renal colic, the development of chronic kidney failure, mineral and bone disorders, and the crucial decision of initiating pharmacological treatment. In the guidelines of the European Association of Urology (EAU) and the American Urological Association (AUA), patients are typically categorized into low- and high-risk stone formers. This classification takes into account a range of factors, including the timing of stone formation, stone composition, stone burden, the presence of (genetic) conditions associated with stone formation, medication history, anatomical anomalies, and environmental and occupational influences [27, 28].

To predict stone recurrence, Rule et al. developed a recurrence of kidney stones (ROKS) nomogram. This predictive tool relies on thirteen readily accessible features from a patient's clinical history, which are typically available at the time of the initial stone episode [29]. Performance of the ROKS nomogram has demonstrated a limited to modest ability in foreseeing stone-related events [30, 31]. Based on a survey on risk estimation of stone recurrence, clinicians seemed not be able to distinguish patients with high and low recurrence risk when compared with peers and the ROKS nomogram [32].

In conclusion, there exists a clear need for additional clinical tools within the healthcare workflow to optimize the precision of stratifying individuals as low or high-risk stone formers. Moreover, it is imperative to explore tailored approaches regarding the type and frequency of imaging, specifically aligned with individual patient risk profiles, to curtail the risks associated with costly and excessive radiation exposure [33, 34].

Etiology of formation

Another method of classifying stones involves categorizing them based on their etiology that can be stratified into four

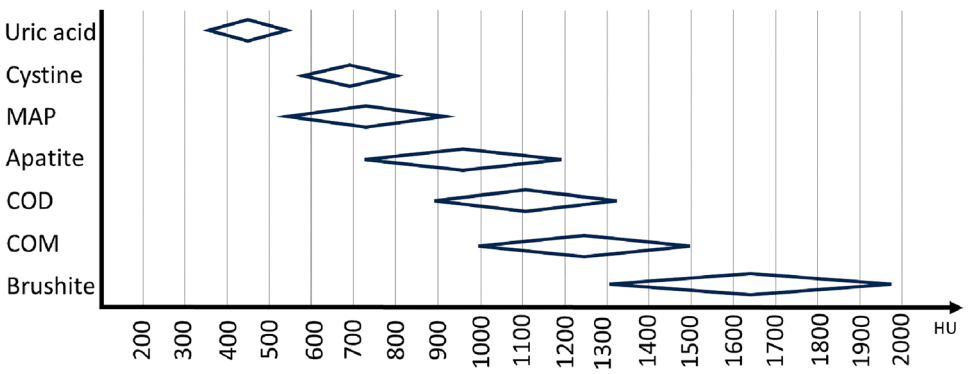

Fig. 2 Stone composition in function of Hounsfield Units on CT in the range of 80 kV to 140 kV *COM* calcium oxalate monohydrate, *COD* calcium oxalate

groups [27]. Stones associated with non-infectious origins, encompassing compositions like calcium oxalate, calcium phosphate, uric acid, and ammonium urate. Additionally, there are stones attributed to infections, which encompass magnesium ammonium phosphate and highly carbonated apatite, and various urates. Third, genetic defects can give rise to stones composed of cystine, xanthine, and 2,8-dihydroxyadenine. Finally, certain stones are linked to the use of specific medications.

Composition

Stones are generally stratified upon composition to distinguish the variations in structure among various stone constitutions and their associated lithogenic processes. In routine clinical practice, diverse techniques are used to analyze stone composition: microscopy (binocular, polarized light and scanning electron microscopy) and constituent analysis (Fourier transform infrared spectroscopy with or without attenuated total reflectance, Raman spectroscopy, X-ray diffraction, and thermal analysis) [35–41].

Microscopic examination is a valuable tool for understanding various aspects of crystalline components, such as their nature, shape, internal structure, and location. It also provides insights into crystalline conversions and the relationships between different crystalline species. This technique has been extensively used to explore the inner structure of stones and reveal the morphology of small crystals [42, 43]. It is worth mentioning that following laser lithotripsy, there has been an observed alteration in the crystalline organization of stone dust when compared to stone fragments [44]. Following Ho:YAG laser lithotripsy, these changes included the conversion of calcium oxalate dihydrate to calcium oxalate monohydrate, shifts in the carbapatite spectra toward an amorphous phase, alterations of magnesium ammonium phosphate toward different amorphous and crystalline phases, and the presence of hydroxyapatite on brushite fragments. On the other hand, after thulium fiber laser lithotripsy, most stone dust samples showed changes in their crystalline organization, with the exception of calcium oxalate monohydrate and carbapatite [45].

Regarding constituent analysis, infrared spectroscopy is currently the reference method. It has a high sensitivity to detect scarce but clinically important components. It also identifies mineral and organic components, drugs, and foreign particles [42]. Until now, there has been no approved standard for conducting stone analysis. Several groups have noticed a strong variability in both qualitative and quantitative stone analysis results among different laboratories and a lack of standardization of used nomenclature [46, 47]. This can be explained by the fact that less than 10% of stones are pure or include only one chemical compound [48]. Since the constituent analyses do not identify stone structure and crystal phases, another technique called morphoconstitutional analysis is of interest to provide information of the lithogenic process of the entire stone.

Morphoconstitutional analysis

The initial endeavor to establish a morphoconstitutional classification of stones was undertaken by Ord and Shattock in 1895[49]. Afterward, multiple groups investigated relationships between stone characteristic and their composition [50–52]. Later, several authors attempted to correlate stone composition with etiopathogenesis [53–56]. In 1993, Daudon et al. provided a detailed understanding of the overall characteristics of urinary stones in their morphoconstitutional analysis [42]. It involves a combined approach to examine both the stone's morphologic appearance and its chemical composition examined with infrared spectroscopy [57]. On the one hand, their refined morphological and structural examination involves observing the stone's size, shape, surface features, and internal organization under optical microscopy including location of different components and crystalline conversion. Compositional analysis using infrared spectroscopy, on the other hand, helps identifying stone composition and to determine the ratio of different components within a single stone [42].

By employing morphoconstitutional analysis, Daudon et al. proposed a classification based on surface and section morphology with its corresponding pathophysiological factors aiding to a better understanding of stone-related diseases and their etiopathogenesis (Table 2, adapted from [58]). They classified stones into seven types and twenty-two subtypes. Each subtype exhibits correlations with specific pathophysiologic conditions, which provides valuable insights into the underlying causes of stone formation and may guide clinicians in the selection of treatment modalities [42, 57, 58]. A series of clinical applications derived from morphoconstitutional analysis are detailed hereunder.

Fast identification of crystalline phase principles

Various chemical components can crystallize in multiple forms. For instance, calcium oxalate can manifest as calcium oxalate monohydrate, calcium oxalate dihydrate, or calcium oxalate trihydrate. As early as four decades ago, research revealed that calcium oxalate monohydrate is influenced by oxalate concentration, while calcium oxalate dihydrate is more dependent on calcium concentration. These diverse crystalline forms have been linked to specific biochemical conditions causing hyperoxaluria and hypercalciuria, respectively [59–61].

Detection of crystalline conversion process

Calcium oxalate dihydrate stones are primarily linked to hypercalciuria, while calcium oxalate monohydrate stones

Table 1 Classification system

Classification System	Application	Interest
Anatomical position	Pyelocaliceal system (renal pelvis, upper, middle, and lower calyces)	Pivotal role in selecting appropriate treatment modalities, ranging from conservative approaches to surgical intervention
	Ureter (ureteropelvic junction, proximal, middle, distal ureter, vesicoureteric junction)	
	Bladder	
	urethra	
Size	One dimension: US, KUB, CT	Unidimensional measurement: adequate for the description of small particles
	Two dimensions: US, KUB, CT	Surface area: more accurate than unidimensional
	Three dimensions: CT	Volume: most accurate method for reporting stone burden. Allows assessment of stone ablation efficiency during laser lithotripsy. Pushes boundaries of retrograde intrarenal surgery for larger stones
Medical imaging characteristics	US	Urolithiasis detection
	KUB: radiopaque or radiolucent	Guiding treatment modalities and follow-up after treatment
	CT: Hounsfield Unit	Predictive capabilities for determining stone compositions. Assessing success rates of treatment modalities. Potential of radiomics
Risk of recurrence	Low- and high-risk stone formers	Safeguarding patients from potential regrowth, episodes of renal colic, the development of chronic kidney failure, mineral and bone disorders, and the decision of initiating pharmacological treatment
	Nomograms	Foreseeing stone-related events. Troublesome application
Etiology of formation	Non-infectious stones	Calcium oxalate, calcium phosphate, uric acid, and ammonium urate
	Infectious stones	Magnesium ammonium phosphate, highly carbonated apatite, various urates
	Genetic stones	Cystine, xanthine, 2,8-dihydroxyadenine
	Other	
Composition	Microscopy	Nature, shape, internal structure, and location of crystalline components. Crystalline conversions. Relationships between different crystalline species
	Constituent analysis	Identification mineral and organic components (but strong variability, and no identification of stone structure and crystal phases)
Morphoconstitutional analysis	Cfr. Figure 1	Fast identification of crystalline phase principles
		Detection of crystalline conversion process
		Directing etiopathogenesis
		Identification of lithogenic process: papillary umbilication and randall plaques
		Assessment of crystal formation speed and recurrence rates
		Guidance of treatment modalities

are predominantly formed due to primary crystallization in hyperoxaluric conditions [57, 62]. Nevertheless, the latter can also arise from the conversion (dehydration) from calcium oxalate dihydrate toward calcium oxalate monohydrate stones [43]. It is crucial to detect this conversion process from calcium oxalate dihydrate to calcium oxalate monohydrate during morphoconstitutional analysis when establishing connections between stone morphology, crystalline composition, and potential etiopathogenic factors.

Directing etiopathogenesis

The refined morphologic examination proposed by Daudon et al. provides etiopathogenic orientations and guides metabolic evaluation [42, 57, 63]. Just to choose one are the carbapatite (calcium phosphate) stones, which account for 10% to 15% of all stones. Based on 1093 patients who had an available etiological diagnosis and stones containing at least 70% of calcium phosphate without magnesium

ammonium phosphate, Dessombz et al. evaluated the stone morphology [64]. They found that 13% of carbapatite stones had a peculiar morphology termed type IVa2, characterized by a smooth aspect and a glazed brown yellow appearance with tiny cracks. Type IVa2 morphology was associated with inherited distal renal tubular acidosis (dRTA) in 53% of cases, medullary sponge kidney in 35%, Sjögren syndrome in 9%, carbonic anhydrase inhibitors intake in 1.5% and urinary tract infection in 1.5%. In contrast, these diseases were associated with IVa1 stones in 0.3%, 17%, 0.7%, 5%, and 40% of cases, respectively. Remarkably, 96% of patients with inherited distal renal tubular acidosis had stone morphology type IVa2, representing a sensitivity and specificity of 96% and 94%, respectively.

Identification of lithogenic process: papillary umbilication and Randall plaques

In 1936, the American urologist Alexander Randall described the presence of calcium phosphate deposits at the tip of the renal papilla. He also observed calcium oxalate renal stones connected to the plaques and put forward the hypothesis that these papillary calcifications could potentially be the initial trigger for stone formation in these patients [65, 66]. Recently, it was found that these plaques have a 83% prevalence in kidney stone formers [67]. The origin of Randall's plaque is thought to be the basement membranes of the thin limbs of the loop of Henle. This plaque formation may be linked to increased calcium reabsorption from the proximal tubule, leading to higher concentrations of calcium in the descending vasa recta and subsequently in the interstitium around thin limbs [68]. These plaques may be influenced by hypercalciuria, and the combined use of vitamin D and calcium could accelerate their formation [69]. Stones that grow over Randall plaques can dislodge and extract a piece of the papilla, creating a visible papillary pit or umbilication. This phenomenon results in a Randall plaque forming on the lower surface of the stone and a papillary pit corresponding to the area of attachment. In 2019, Almeras et al. introduced a classification system for renal papillary abnormalities visualized during flexible ureteroscopy with the aim of standardizing their description. This classification, denoted as Sx nPx Drx/i/px, comprises various elements: S designates the observed type of papillary stones, n denotes the count of abnormal papillae within the same kidney along with their specific type (P), and D encompasses deposits, which includes quantification of Randall's plaques (rx), as well as the presence of active intrapapillary papular deposits (i) and plugs (p) [67]. This observation has the potential to contribute to our understanding of nephrolithogenesis mechanisms and the risk of stone recurrence [70].

Assessing the stone surface can also be used to track other stones. Similar to beach pebbles, certain stones types (such as Id, IIc, IIIa, Vb) display distinct characteristics with smooth, rounded, and naturally polished surfaces. This appearance is a result of constant mechanical interaction, as the stones continuously toss and roll against each other, leading to abrasion and surface smoothing. This particular morphology indicates the presence of multiple stones and conditions of stasis, such as calyceal diverticulum, ureteropelvic junction stenosis, and benign prostatic obstruction [42, 58].

Assessment of crystal formation speed

Crystal formation speed and recurrence rates are important clinical parameters that may hint to the underlying metabolic disease. A typical example is primary hyperoxaluria, which is an uncommon genetic disorder that results in an excessive production of oxalate, mainly affecting the kidneys and resulting in fast growth of calcium oxalate monohydrate stones. To prevent complications and preserve kidney function, early diagnosis and intervention are essential [71]. A study conducted by Daudon et al. involved the stone analysis of 74 patients with primary hyperoxaluria. They discovered a distinct stone morphology within this group. The stones exhibited a whitish or pale-yellow surface and a loose, unorganized inner structure (type Ic), which was notably different from the dark-brown surface and well-organized, radiating inner structure (type Ia) commonly seen in most calcium oxalate monohydrate stones. Scanning electron microscopy confirmed that the crystalline structure found in the primary hyperoxaluria stones (type Ic) was different from the typical structure observed in the common whewellite stone (type Ia). The authors hypothesized that this dissimilarity in morphology is indicative of the rapid and permanent crystal formation induced by genetic hyperoxaluria. They concluded that this peculiar stone morphology is pathognomonic for primary hyperoxaluria and should prompt an early and comprehensive laboratory evaluation [72, 73]. If morphological analysis was omitted, patients with primary hyperoxaluria may suffer from delayed time point of diagnosis and impaired kidney function.

Assessment of recurrence rates

Guidelines of EAU and AUA recommend close follow-up and metabolic testing in recurrent stone formers [27, 28]. This assessment considers particular stone compositions, including brushite, uric acid, urate, and cystine. Recently, Daudon et al. assessed the risk of recurrency based on the morphoconstitutional analysis of 38,274 stones [74]. The age of first stone occurrence varied, with dihydroxyadenine occurring at the youngest age (15.7 years) and anhydrous uric acid at the

oldest (62.5 years). Calcium oxalate stones fell in between (40.7 years for calcium oxalate dihydrate and 48.4 years for calcium oxalate monohydrate). When considering composition alone, calcium oxalate monohydrate stones had a lower recurrence rate, with only 38.0% coming from patients with previous episodes. However, when examining different calcium oxalate monohydrate morphologies, type Ic had a significantly higher recurrence rate (82.4%). Similarly, among stones composed of apatite, type IVa2 had a higher recurrence rate compared to other apatite morphologies (78.8% vs. 39–42%). They concluded that stone composition alone is insufficient to predict recurrence risk, and considering stone morphology can aid in identifying highly recurrent stones.

Guidance of treatment modalities

Initially, it was thought that resistance to SWL was related to crystalline compositions [75]. It was only after later research that stone fragility was found to be associated with stone mineral content measured by dual photon absorptiometry [76, 77]. Williams et al. found that the variability in stone fragility to shock waves was large within groups of the same mineral composition. They hypothesized that the variation in stone structure could underlie the variation in stone fragility within the same stone composition [78]. This was further analyzed by Daudon et al. on several morphologies of calcium oxalate monohydrate stones [42]. To gain a deeper understanding of the crystalline structure, a single-crystal neutron study was conducted using a four-circle automated diffractometer. Additionally, scanning electron microscopy was employed to investigate the mesoscopic scale, while powder neutron diffraction was used to explore the nanometric scale. All types of whewellite stones showed a similar structure at the nanometric scale. However, significant differences were observed at the mesoscopic scale. The study revealed a close relationship between stone morphology and the organization of the crystals at the mesoscopic level, which also had an impact on the effectiveness of SWL. From an analysis involving 1270 SWL procedures performed on calcium oxalate monohydrate stones (including type Ia, Ib, and Id), the failure rates were found to be 80% for type Ib stones; whereas for type Ia and Id stones, the failure rates were less than 10% [79]. This research provided valuable insights into the morphological and structural characteristics of different types of whewellite stones, shedding light on the association between their formation and response to SWL. These findings were in line with prior studies showing higher success rates for smooth surfaced stones compared to rough surfaced stones [80, 81]. In conclusion, the resistance to fragmentation by shock waves appears to be more related to the organization of the stones, particularly for poorly organized structures (e.g., type Ib and Va), rather than their stone composition.

Discussion

Stones can be classified according to various criteria such as anatomical position, size, medical imaging features, risk of recurrence, etiology, composition, and morphoconstitutional analysis (Table 1). Categorizing stones by anatomical position, size, and medical imaging characteristics is a straightforward process that can arguably directly impact treatment recommendations. Given that CT imaging is typically administered prior to treatment for most patients, determining the precise anatomical location, stone dimensions, and HU can be easily interpreted and should be recommended (expert opinion). In the process of offering treatment modalities such as SWL, RIRS, or PNCL, these criteria must be considered in conjunction with patient preferences. Radiomics, the utilization of artificial intelligence capabilities within the domain of medical imaging, has the potential to enhance this personalized patient approach [26].

In contrast, the classification of stones according to risk of recurrence and etiology is more complex since it depends on multiple variables, including stone composition and morphology. Importantly, the composition of most kidney stones is typically mixed [82–84]. This can arise from the presence of concurrent lithogenic factors on one hand, or from subsequent conditions triggering new lithogenic processes, such as dietary hyperoxaluria, dietary hypercalciuria, gout, diabetes mellitus, chronic diarrhea, abuse of laxatives, primary hyperparathyroidism, intake of carbonic anhydrase inhibitors, or urinary tract infections. As stones are infrequently extracted in one piece since the advent of minimally invasive techniques, it becomes crucial to identify the structural characteristics of stone surfaces and sections (including judgement of stone core localization, e.g., Randall plaque) during surgery [42, 57, 58, 63]. This is particularly important since stone composition can alter during laser lithotripsy [44, 45, 85]. Consequently, the stone dust generated might not adequately represent the crystalline organization of the stones before laser lithotripsy. To address this, Estrade et al. evaluated the feasibility of intra-operative stone composition recognition by a single expert urologist using Daudon et al. morphoconstitutional classification [42, 86]. They discovered an 82% agreement between endoscopic and microscopic characterizations of urinary stones. In contrast, Henderickx et al. also assessed the diagnostic accuracy and intra-observer agreement of endoscopic stone recognition compared to formal stone analysis by fifteen urologists. They concluded that diagnostic accuracy was limited, and intra-observer agreement fell below an acceptable threshold [87]. One possible solution lies in utilizing automated computer-assisted in situ recognition of morphological characteristics of both pure and mixed urinary stones, as demonstrated in a preliminary study with promising discrimination results

Table 2 Morphoconstitutional analysis of urinary calculi (adapted from [42 and 58])

Type	Subtype	Composition	Frequency (%)*	Surface	Section	Etiology
I	Ia	Whewellite	45	Brown; smooth, mammillary or mulberry shaped; frequent umbilication	Brown; compact, concentric structure, radial crystallization	Diet hyperoxaluria, medullary sponge kidney, Randall plaques
	Ib	Whewellite	7	Beige to dark brown; mammillary and rough	Dark brown; compact with some gaps, unorganized	Hyperoxaluria, stasis, crystalline conversion
	Ic	Whewellite	0.4	Cream to light brown; smooth or granular	Beige; compact, finely granular, unorganized	Primary hyperoxaluria
	Id	Whewellite	1.6	Pale brown; smooth	Beige; compact, microcrystalline structure, thin concentric layers	Malformative uropathy, stasis, multiple stones
	Ie	Whewellite	0.5	Beige; mammillary or granular	Beige; powdery, unorganized	Enteric hyperoxaluria, short bowel
II	IIa	Weddellite	30	Yellowish-brown; spiculate, entanglement of bipyramidal crystals	Yellowish-brown; crystalline, radial crystallization	Hypercalciuria
	IIb	Weddellite ± whewellite	22	Yellowish-brown; spiculate, entangled pyramidal crystals, blunt edges	Yellowish-brown; compact, crystalline, unorganized	Hypercalciuria ± hyperoxaluria, stasis, crystalline conversion
	IIc	Weddellite	0.1	Gray–beige to dark yellow–brown; rough, microcrystalline	Dark yellow–brown; peripheral diffuse concentric, core loose unorganized	Hypercalciuria, malformative uropathy stasis, multiple stones
III	IIIa	Anhydrous uric acid	2	Ocher or gray–beige; homogeneous, crystalline, smooth or slightly embossed	Ocher; compact concentric structure, radial crystallization	Hyperuricosuria, acid ph, stasis
	IIIb	Dihydrate uric acid ± anhydrous	9	Whitish to brownish-red; heterogeneous, locally crystalline, rough or porous	Orange; compact or loosely crystalline, unorganized structure, porous areas	Renal ammoniagenesis defect, hyperuricemia, hyperuricosuria, gout, diabetes mellitus, metabolic syndrome, diarrhea, candidiasis, myelo- and lymphoproliferative diseases
	IIIc	Various urates	1.1	Whitish to gray–brown; heterogeneous, rough, locally porous, microcrystalline	Gray–brown; compact, microcrystalline, unorganized	Hyperuricosuria, alkaline ph (iatrogenic, UTI)
	IIId	Ammonium urate	0.2	Grayish to brown; heterogeneous, microcrystalline, rough and extensively porous	Gray–brown; heterogeneous, loose concentric layers (thick brown/thin beige), locally porous	Hyperuricosuria, renal or urinary hyperammoniagenesis, phosphorus deficiency, digestive alkali loss (chronic infectious diarrhea, laxative abuse) malnutrition, anorexia nervosa
IV	IVa1	Carbapatite	30	Whitish to beige; homogeneous, crystalline, rough, finely embossed	Beige; homogeneous, microcrystalline, crumbly ± concentric structure	UTI, hypercalciuria with incomplete renal tubular acidosis, primary hyperparathyroidism, secondary renal tubular acidosis (e.g., acetazolamide)
	IVa2	Carbapatite	1.6	Brown–yellow; heterogeneous embossed, crystalline, glazed, irregular shape	Heterogeneous concentric foliated. Thick brown–yellow layers and thin microcrystalline beige layers	Primary (e.g., Albright) or acquired (e.g., Sjögren) distal renal tubular acidosis, UTI, medullary sponge kidney
	IVb	Carbapatite ± struvite	6	Whitish to brown; heterogeneous, both rough and embossed	Heterogeneous concentric with thick whitish and thin brown–yellow layers	Primary hyperparathyroidism, hypercalciuria and hyperphosphaturia, UTI

Table 2 (continued)

Type	Subtype	Composition	Frequency (%)*	Surface	Section	Etiology
	IVc	Struvite	2.5	White; homogeneous, crystalline, amalgamate crystals with blunt edges	White; loose, radial crystallization, sometimes diffuse concentric organization	UTI
	IVd	Brushite	1.7	Whitish to beige. Homogeneous, crystalline, finely rough or dappled, slightly translucent	White–beige; Compact concentric layers with radial crystallization	Hypercalciuria and hyperphosphaturia, primary hyperparathyroidism, medullary sponge kidney, sarcoidosis, phosphate diabetes, distal renal tubular acidosis
V	Va	Cystine	1.1	Brown–yellow; homogeneous, crystalline, granular or embossed, waxy aspect	Yellow–pale brown; homogeneous, unorganized, diffuse radial crystallization	Cystinuria
	Vb	Cystine	0.2	White, beige, brown–yellow; homogeneous, microcrystalline, smooth	Yellow–brown; homogeneous, compact, whitish thin concentric layers in periphery, unorganized core	Cystinuria with inadequate therapy, malformative uropathy, stasis, multiple stones
VI	VIa	Proteins	0.7	White to pale brown; soft, homogeneous, smooth, unorganized, translucent	White–pale brown; homogeneous, unorganized, foci of secondary mineralization	Chronic pyelonephritis
	VIb	Proteins + medication or metabolic derivatives	5	Brown to black; heterogeneous, irregularly rough, locally scaled	Brown blended with color of associated components; heterogeneous, slightly organized	Proteinuria, hematuria, drugs
	VIc	Proteins and whewellite	0.1	Brown to black; homogeneous, smooth with clefts and scales	Yellow–brown; homogeneous, unorganized, loose, brown or heterogeneous with brown proteic shield surrounding a loose core	End stage renal failure, hemodialysis with calcium/vitamin D supplements

*Cumulative for pure and mixed form

UTI urinary tract infection

[88]. Incorporating specialized artificial intelligence into ureteroscopes may represent a significant advancement toward perioperative morphoconstitutional analysis [89–91].

Currently, the guidelines of the EAU and the AUA primarily propose treatment algorithms based on the stone's anatomical position and size as a unidimensional measurement. However, considering all three dimensions would offer a more accurate assessment of stone burden and could assist urologists in selecting treatment modalities based on their individual stone ablation efficiency. When implementing this approach, the incorporation of other aforementioned classifications, including medical imaging characteristics and patients' medical history, could further aid in the appropriate selection of treatments and the assessment of success rates in everyday practice [92]. Moreover, the inclusion of morphoconstitutional analysis could significantly enhance the management of urolithiasis patients. This analysis allows for the rapid identification of crystalline phase principles, the detection of crystalline conversion processes, the determination of etiopathogenesis, the recognition of lithogenic processes, the assessment of crystal formation speed, and the evaluation of recurrence rates, and the guidance for selecting appropriate treatment modalities. Therefore, as no single classification system can cover all aspects comprehensively, the integration of all classification approaches is essential for tailoring a patient-specific treatment approach.

Conclusion

Classification of urinary stones involves several criteria, each offering unique insights into stone characteristics and formation. Anatomical position, stone size, and medical imaging characteristics provide essential information for treatment decisions. Classification based on risk of recurrence and etiology is more complex, demanding a comprehensive understanding of stone composition and morphology. The use of advanced techniques like morphoconstitutional analysis, which is rapid and low cost by combining morphological appearance and chemical composition, has proven invaluable in identifying stone-related diseases and guiding treatment strategies. This holistic approach has enabled the identification of distinct crystalline phases, determination of lithogenic processes, and even tracking stone history. Becoming familiar with and combining all these classification systems will assist urologists in refining personalized clinical management approaches. Furthermore, as technology continues to evolve, the integration of automated stone recognition and artificial intelligence holds promising potential for enhancing stone recognition accuracy and for integrating all the described stone classifications, further aiding urologists in adopting a tailored approach.

Acknowledgements Our special thanks go to Michel Daudon (Laboratoire des Lithiases, Service des Explorations Fonctionnelles Multidisciplinaires, AP-HP, Hôpital Tenon, Paris, France) for proofreading this article.

Author contributions VDC: protocol/project development, data collection or management, data analysis, manuscript writing/editing. AS: protocol/project development, manuscript writing/editing. PJ-J: manuscript writing/editing. MJ: manuscript writing/editing. OT: research concept, protocol/project development. EXK: research concept, protocol/project development, data collection or management, data analysis, manuscript writing/editing.

Funding None.

Declarations

Conflict of interest Vincent De Coninck is a speaker and/or consultant for BD, Coloplast, and Karl Storz, and has no specific conflicts relevant to this study. Andreas Skolarikos is a consultant for Boston Scientific, and has no specific conflicts relevant to this study. Olivier Traxer is a consultant for Coloplast, Karl Storz, Rocamed, Quanta Systems, Ambu, Boston Scientific, and IPG Medical, and has no specific conflicts relevant to this study. Etienne Xavier Keller is a speaker and/or consultant for Coloplast, Olympus, Boston Scientific, Recordati, Debiopharm and Alnylam, and has no specific conflicts of interest relevant to this work. All other authors have no conflicts of interest.

Ethical approval Not applicable.

References

1. Sorokin I, Mamoulakis C, Miyazawa K, Rodgers A, Talati J, Lotan Y (2017) Epidemiology of stone disease across the world. World J Urol 35:1301–1320
2. Lang J, Narendrula A, El-Zawahry A, Sindhwani P, Ekwenna O (2022) Global Trends in Incidence and Burden of Urolithiasis from 1990 to 2019: An Analysis of Global Burden of Disease Study Data. Eur Urol Open Sci 35:37–46
3. Juliebo-Jones P, Ulvik O, Ms AE, Gjengsto P, Beisland C, Somani BK (2023) Mortality due to urolithiasis in England and Wales: updated findings from a national database over a 23-year period. Cent Eur J Urol 76:141–143
4. Assimos D, Krambeck A, Miller NL, Monga M, Murad MH, Nelson CP et al (2016) Surgical Management of Stones: American Urological Association/Endourological Society Guideline. PART II J Urol 196:1161–1169
5. Geraghty RM, Davis NF, Tzelves L, Lombardo R, Yuan C, Thomas K et al (2023) Best Practice in Interventional Management of Urolithiasis: An Update from the European Association of Urology Guidelines Panel for Urolithiasis 2022. Eur Urol Focus 9:199–208
6. Keller EX, De Coninck V, Traxer O, Shvero A, Kleinmann N, Hubosky SG, et al. Stones. Advanced Ureteroscopy: A Practitioner's Guide to Treating Difficult Problems: Springer; 2021. p. 105–54
7. Keller EX, De Coninck V, Audouin M, Doizi S, Daudon M, Traxer O (2019) Stone composition independently predicts stone size in 18,029 spontaneously passed stones. World J Urol 37:2493–2499

8. De Coninck V, Antonelli J, Chew B, Patterson JM, Skolarikos A, Bultitude M (2019) Medical Expulsive Therapy for Urinary Stones: Future Trends and Knowledge Gaps. Eur Urol 76:658–666
9. De Coninck V, Traxer O (2018) The Time Has Come to Report Stone Burden in Terms of Volume Instead of Largest Diameter. J Endourol 32:265–266
10. Keller EX, De Coninck V, Doizi S, Daudon M, Traxer O (2021) What is the exact definition of stone dust? An in vitro evaluation. World J Urol 39:187–194
11. De Coninck V, Ventimiglia E, Traxer O (2022) How Should We Assess Stone Ablation Efficacy When Comparing Different Lasers? Eur Urol Focus 8:1450–1451
12. De Coninck V, Somani B, Sener ET, Emiliani E, Corrales M, Juliebo-Jones P et al (2022) Ureteral access sheaths and its use in the future: a comprehensive update based on a literature review. J Clin Med 11(17):5128
13. Keller EX, De Coninck V, Doizi S, Traxer O (2020) The role of ureteroscopy for treatment of staghorn calculi: A systematic review. Asian J Urol 7:110–115
14. Elton DC, Turkbey EB, Pickhardt PJ, Summers RM (2022) A deep learning system for automated kidney stone detection and volumetric segmentation on noncontrast CT scans. Med Phys 49:2545–2554
15. Rodriguez-Plata IT, Medina-Escobedo M, Basulto-Martinez M, Avila-Nava A, Gutierrez-Solis AL, Mendez-Dominguez N et al (2021) Implementation of a Technique Based on Hounsfield Units and Hounsfield Density to Determine Kidney Stone Composition. Tomography 7:606–613
16. Tailly T, Larish Y, Nadeau B, Violette P, Glickman L, Olvera-Posada D et al (2016) Combining Mean and Standard Deviation of Hounsfield Unit Measurements from Preoperative CT Allows More Accurate Prediction of Urinary Stone Composition Than Mean Hounsfield Units Alone. J Endourol 30:453–459
17. Kaviani P, Primak A, Bizzo B, Ebrahimian S, Saini S, Dreyer KJ et al (2023) Performance of threshold-based stone segmentation and radiomics for determining the composition of kidney stones from single-energy CT. Jpn J Radiol 41:194–200
18. Euler A, Wullschleger S, Sartoretti T, Muller D, Keller EX, Lavrek D et al (2023) Dual-energy CT kidney stone characterization-can diagnostic accuracy be achieved at low radiation dose? Eur Radiol 33(9):6238–6244
19. Grosjean R, Sauer B, Guerra RM, Daudon M, Blum A, Felblinger J et al (2008) Characterization of human renal stones with MDCT: advantage of dual energy and limitations due to respiratory motion. AJR Am J Roentgenol 190:720–728
20. Bellin MF, Renard-Penna R, Conort P, Bissery A, Meric JB, Daudon M et al (2004) Helical CT evaluation of the chemical composition of urinary tract calculi with a discriminant analysis of CT-attenuation values and density. Eur Radiol 14:2134–2140
21. Mostafavi MR, Ernst RD, Saltzman B (1998) Accurate determination of chemical composition of urinary calculi by spiral computerized tomography. J Urol 159:673–675
22. Tsaturyan A, Bokova E, Bosshard P, Bonny O, Fuster DG, Roth B (2020) Oral chemolysis is an effective, non-invasive therapy for urinary stones suspected of uric acid content. Urolithiasis 48:501–507
23. Garg M, Johnson H, Lee SM, Rai BP, Somani B, Philip J (2023) Role of Hounsfield Unit in Predicting Outcomes of Shock Wave Lithotripsy for Renal Calculi: Outcomes of a Systematic Review. Curr Urol Rep 24:173–185
24. Joseph P, Mandal AK, Singh SK, Mandal P, Sankhwar SN, Sharma SK (2002) Computerized tomography attenuation value of renal calculus: can it predict successful fragmentation of the calculus by extracorporeal shock wave lithotripsy? A preliminary study J Urol 167:1968–1971
25. Perks AE, Gotto G, Teichman JM (2007) Shock wave lithotripsy correlates with stone density on preoperative computerized tomography. J Urol 178:912–915
26. Lim EJ, Castellani D, So WZ, Fong KY, Li JQ, Tiong HY, et al. (2022) Radiomics in Urolithiasis: Systematic Review of Current Applications, Limitations, and Future Directions. J Clin Med 11(17):5151
27. Skolarikos A, Neisius A, Petřík A, Somani B, Thomas K, Gambaro G, et al. (2022) Urolithiasis. EAU Guidelines Edn presented at the EAU Annual Congress Amsterdam
28. Pearle MS, Goldfarb DS, Assimos DG, Curhan G, Denu-Ciocca CJ, Matlaga BR et al (2014) Medical management of kidney stones: AUA guideline. J Urol 192:316–324
29. Rule AD, Lieske JC, Li X, Melton LJ 3rd, Krambeck AE, Bergstralh EJ (2014) The ROKS nomogram for predicting a second symptomatic stone episode. J Am Soc Nephrol 25:2878–2886
30. Kavoussi NL, Da Silva A, Floyd C, McCoy A, Koyama T, Hsi RS (2023) Feasibility of stone recurrence risk stratification using the recurrence of kidney stone (ROKS) nomogram. Urolithiasis 51:73
31. Iremashvili V, Li S, Penniston KL, Best SL, Hedican SP, Nakada SY (2019) External Validation of the Recurrence of Kidney Stone Nomogram in a Surgical Cohort. J Endourol 33:475–479
32. Forbes CM, McCoy AB, Hsi RS (2021) Clinician Versus Nomogram Predicted Estimates of Kidney Stone Recurrence Risk. J Endourol 35:847–852
33. Rodger F, Roditi G, Aboumarzouk OM (2018) Diagnostic Accuracy of Low and Ultra-Low Dose CT for Identification of Urinary Tract Stones: A Systematic Review. Urol Int 100:375–385
34. Brisbane W, Bailey MR, Sorensen MD (2016) An overview of kidney stone imaging techniques. Nat Rev Urol 13:654–662
35. Snicorius M, Drevinskaite M, Miglinas M, Cekauskas A, Stadulyte M, Bandzeviciute R et al (2023) A Novel Infrared Spectroscopy Method for Analysis of Stone Dust for Establishing Final Composition of Urolithiasis. Eur Urol Open Sci 47:36–42
36. Castiglione V, Sacre PY, Cavalier E, Hubert P, Gadisseur R, Ziemons E (2018) Raman chemical imaging, a new tool in kidney stone structure analysis: Case-study and comparison to Fourier Transform Infrared spectroscopy. PLoS ONE 13:e0201460
37. Khan AH, Imran S, Talati J, Jafri L (2018) Fourier transform infrared spectroscopy for analysis of kidney stones. Investig Clin Urol 59:32–37
38. Racek M, Racek J, Hupakova I (2019) Scanning electron microscopy in analysis of urinary stones. Scand J Clin Lab Invest 79:208–217
39. Daudon M, Jungers P, Lacour B (2004) Clinical value of crystalluria study. Ann Biol Clin (Paris) 62:379–393
40. Daudon M (1991) Jungers P [Analytical methods of calculi and urinary crystals]. Rev Prat 41:2017–2022
41. Zhu W, Sun Z, Ye L, Zhang X, Xing Y, Zhu Q et al (2022) Preliminary assessment of a portable Raman spectroscopy system for post-operative urinary stone analysis. World J Urol 40:229–235
42. Daudon M, Bader CA, Jungers P (1993) Urinary calculi: review of classification methods and correlations with etiology. Scann Microsc 7:1081–1104
43. De Coninck V, Keller EX, Daudon M, Traxer O (2019) RE: Geobiology reveals how human kidney stones dissolve in vivo (by: Sivaguru et al 2018). World J Urol 37:2543
44. Keller EX, de Coninck V, Audouin M, Doizi S, Bazin D, Daudon M et al (2019) Fragments and dust after Holmium laser lithotripsy with or without "Moses technology": How are they different? J Biophotonics 12:e201800227
45. Keller EX, De Coninck V, Doizi S, Daudon M, Traxer O (2021) Thulium fiber laser: ready to dust all urinary stone composition types? World J Urol 39:1693–1698

46. Krambeck AE, Khan NF, Jackson ME, Lingeman JE, McAteer JA, Williams JC Jr (2010) Inaccurate reporting of mineral composition by commercial stone analysis laboratories: implications for infection and metabolic stones. J Urol 184:1543–1549
47. Siener R, Buchholz N, Daudon M, Hess B, Knoll T, Osther PJ et al (2016) Quality Assessment of Urinary Stone Analysis: Results of a Multicenter Study of Laboratories in Europe. PLoS ONE 11:e0156606
48. Daudon M, Donsimoni R, Hennequin C, Fellahi S, Le Moel G, Paris M et al (1995) Sex- and age-related composition of 10 617 calculi analyzed by infrared spectroscopy. Urol Res 23:319–326
49. Ord WM, Shattock SG (1895) On the microscopic structure of urinary calculi of oxalate of lime: Adlar and Son, Bartholomew Close
50. Prien EL, Frondel C (1947) Studies in urolithiasis: I. The composition of urinary calculi. J Urol 57:949–991
51. Murphy BT, Pyrah L (1962) The composition, structure, and mechanisms of the formation of urinary calculi. Br J Urol 34:129–159
52. Schubert G, Brien G (1981) Crystallographic investigations of urinary calcium oxalate calculi. Int Urol Nephrol 13:249–260
53. Otnes B (1983) Correlation between causes and composition of urinary stones. Scand J Urol Nephrol 17:93–98
54. Pak CY (1991) Etiology and treatment of urolithiasis. Am J Kidney Dis 18:624–637
55. Smith L (1987) Pathogenesis of renal stones. Miner Electrolyte Metab 13:214–219
56. Wilson DM (1989) Clinical and laboratory approaches for evaluation of nephrolithiasis. J Urol 141:770–774
57. Daudon M, Jungers P (2004) Clinical value of crystalluria and quantitative morphoconstitutional analysis of urinary calculi. Nephron Physiol 98:p31–p36
58. De Coninck V, Keller EX, Traxer O (2019) Metabolic evaluation: who, when and how often. Curr Opin Urol 29:52–64
59. Asplin JR, Lingeman J, Kahnoski R, Mardis H, Parks JH, Coe FL (1998) Metabolic urinary correlates of calcium oxalate dihydrate in renal stones. J Urol 159:664–668
60. Daudon M (1984) Reveillaud RJ [Whewellite and weddellite: toward a different etiopathogenesis. The significance of morphological typing of calculi]. Nephrologie 5:195–201
61. von Unruh GE, Voss S, Sauerbruch T, Hesse A (2004) Dependence of oxalate absorption on the daily calcium intake. J Am Soc Nephrol 15:1567–1573
62. Frochot V, Daudon M (2016) Clinical value of crystalluria and quantitative morphoconstitutional analysis of urinary calculi. Int J Surg 36:624–632
63. Cloutier J, Villa L, Traxer O, Daudon M (2015) Kidney stone analysis: "Give me your stone, I will tell you who you are!" World J Urol 33:157–169
64. Dessombz A, Letavernier E, Haymann JP, Bazin D, Daudon M (2015) Calcium phosphate stone morphology can reliably predict distal renal tubular acidosis. J Urol 193:1564–1569
65. Randall A (1936) An Hypothesis for the Origin of Renal Calculus. N Engl J Med 214:234–242
66. Daudon M, Bazin D, Letavernier E (2015) Randall's plaque as the origin of calcium oxalate kidney stones. Urolithiasis 43(Suppl 1):5–11
67. Almeras C, Daudon M, Estrade V, Gautier JR, Traxer O, Meria P (2021) Classification of the renal papillary abnormalities by flexible ureteroscopy: evaluation of the 2016 version and update. World J Urol 39:177–185
68. Evan AP, Coe FL, Lingeman J, Bledsoe S, Worcester EM (2018) Randall's plaque in stone formers originates in ascending thin limbs. Am J Physiol Renal Physiol 315:F1236–F1242
69. Bouderlique E, Tang E, Perez J, Coudert A, Bazin D, Verpont MC et al (2019) Vitamin D and Calcium Supplementation Accelerates Randall's Plaque Formation in a Murine Model. Am J Pathol 189:2171–2180
70. Borofsky MS, Williams JC Jr, Dauw CA, Cohen A, Evan AC, Coe FL et al (2019) Association Between Randall's Plaque Stone Anchors and Renal Papillary Pits. J Endourol 33:337–342
71. Ching CB, Dickinson K, Karafilidis J, Marchesani N, Mucha L, Antunes N et al (2023) The real world experience of pediatric primary hyperoxaluria patients in the PEDSnet clinical research network. Eur J Pediatr 182(9):4027–4036
72. Daudon M, Jungers P, Bazin D (2008) Peculiar morphology of stones in primary hyperoxaluria. N Engl J Med 359:100–102
73. Daudon M, Estepa L, Lacour B, Jungers P (1998) Unusual morphology of calcium oxalate calculi in primary hyperoxaluria. J Nephrol 11(Suppl 1):51–55
74. Daudon M, Jungers P, Bazin D, Williams JC Jr (2018) Recurrence rates of urinary calculi according to stone composition and morphology. Urolithiasis 46:459–470
75. Dretler SP (1988) Stone fragility–a new therapeutic distinction. J Urol 139:1124–1127
76. Sakamoto W, Kishimoto T, Takegaki Y, Sugimoto T, Wada S, Yamamoto K et al (1991) Stone fragility–measurement of stone mineral content by dual photon absorptiometry. Eur Urol 20:150–153
77. Mandhani A, Raghavendran M, Srivastava A, Kapoor R, Singh U, Kumar A et al (2003) Prediction of fragility of urinary calculi by dual X-ray absorptiometry. J Urol 170:1097–1100
78. Williams JC Jr, Saw KC, Paterson RF, Hatt EK, McAteer JA, Lingeman JE (2003) Variability of renal stone fragility in shock wave lithotripsy. Urology 61:1092–1096
79. Daudon M, Bazin D, Andre G, Jungers P, Cousson A, Chevallier P et al (2009) Examination of whewellite kidney stones by scanning electron microscopy and powder neutron diffraction techniques. J Appl Crystallogr 42:109–115
80. Bhatta KM, Prien EL Jr, Dretler SP (1989) Cystine calculi–rough and smooth: a new clinical distinction. J Urol 142:937–940
81. Pittomvils G, Vandeursen H, Wevers M, Lafaut JP, De Ridder D, De Meester P et al (1994) The influence of internal stone structure upon the fracture behaviour of urinary calculi. Ultrasound Med Biol 20:803–810
82. Zreik R, Pilosov Solomon I, Saliba W, Tor R, Cohen S, Friefeld Y et al (2023) The relationship between patients' kidney stone type and demographics in Israel: analysis of 10 K patients. World J Urol 41:1641–1646
83. Daudon M (2005) Epidemiology of nephrolithiasis in France. Ann Urol (Paris) 39:209–231
84. Halinski A, Bhatti KH, Boeri L, Cloutier J, Davidoff K, Elqady A et al (2021) Stone composition of renal stone formers from different global regions. Arch Ital Urol Androl 93:307–312
85. Sierra A, Corrales M, Kolvatzis M, Daudon M, Traxer O (2022) Thulium Fiber Laser's Dust for Stone Composition Analysis: Is It Enough? A Pilot Study J Endourol 36:1468–1474
86. Estrade V, Denis de Senneville B, Meria P, Almeras C, Bladou F, Bernhard JC et al (2021) Toward improved endoscopic examination of urinary stones: a concordance study between endoscopic digital pictures vs microscopy. BJU Int 128:319–330
87. Henderickx M, Stoots SJM, De Bruin DM, Wijkstra H, Freund JE, Wiseman OJ et al (2022) How Reliable Is Endoscopic Stone Recognition? A Comparison Between Visual Stone Identification and Formal Stone Analysis. J Endourol 36:1362–1370
88. Estrade V, Daudon M, Richard E, Bernhard JC, Bladou F, Robert G et al (2022) Towards automatic recognition of pure and mixed stones using intra-operative endoscopic digital images. BJU Int 129:234–242
89. Estrade V, Daudon M, Richard E, Bernhard JC, Bladou F, Robert G et al (2022) Deep morphological recognition of kidney stones

using intra-operative endoscopic digital videos. Phys Med Biol 67 (16)
90. El Beze J, Mazeaud C, Daul C, Ochoa-Ruiz G, Daudon M, Eschwege P et al (2022) Evaluation and understanding of automated urinary stone recognition methods. BJU Int 130:786–798
91. Black KM, Law H, Aldoukhi A, Deng J, Ghani KR (2020) Deep learning computer vision algorithm for detecting kidney stone composition. BJU Int 125:920–924
92. Kwok JL, De Coninck V, Ventimiglia E, Panthier F, Corrales M, Sierra A et al (2023) Laser ablation efficiency, laser ablation speed, and laser energy consumption during lithotripsy: what are they and how are they defined? A systematic review and proposal for a standardized terminology. European Urology Focus S2405–4569(23):00222–00225

Publisher's Note Springer Nature remains neutral with regard to jurisdictional claims in published maps and institutional affiliations.

Springer Nature or its licensor (e.g. a society or other partner) holds exclusive rights to this article under a publishing agreement with the author(s) or other rightsholder(s); author self-archiving of the accepted manuscript version of this article is solely governed by the terms of such publishing agreement and applicable law.